Shear Wave Elasticity by Tracing Total Nodule Showed High Reproducibility and Concordance with Fibrosis Leading to Discrepant Cut-off Values in Thyroid Cancer

Myung Hi Yoo
Soonchunhyang University Hospital
Hye Jeong Kim (eyedr53@gmail.com)
Soonchunhyang University Hospital https://orcid.org/0000-0003-1010-9803
In Ho Choi
Soonchunhyang University Hospital
Suyeon Park
Soonchunhyang University Hospital
Sang Jin Kim
Soonchunhyang University Hospital
Hyeong Kyu Park
Soonchunhyang University Hospital
Dong Won Byun
Soonchunhyang University Hospital
Kyoil Suh
Soonchunhyang University Hospital

Research article

Keywords: Elastography, shear wave, thyroid cancer, fibrosis

Posted Date: July 25th, 2019

DOI: https://doi.org/10.21203/rs.2.11903/v1

Version of Record: A version of this preprint was published on February 12th, 2020. See the published version at https://doi.org/10.1186/s12885-019-6437-z.

Abstract

Background Although shear wave elastography (SWE) is reported to be useful in detecting malignant thyroid nodules, it showed a wide range of cut-off values of elasticity index (EI) in detecting malignant nodules. The cause of discrepancy has not been clarified yet. Fibrosis of the tumors is known to increase the EI in SWE, and matching of SWE and surgical histopathology has not been fully illustrated in thyroid cancer. We aimed to evaluate the reproducibility of the new total nodular region of interest (ROI) method excluding the subjective features of focal circular ROI placement and to determine the lesion that causes the elevation of EI on SWE and on histopathology. Methods A total of 29 thyroid cancers from 28 patients were included. We evaluated the reproducibility of EI in the new total nodular ROI using Q-Box Trace program and compared the EI in focal nodular ROI using a 3-mm circular area. We analyzed the correlation between fibrosis and EI. Result The coefficient of variation (CV) of the intrarater assay was significantly lower in total nodular ROI than in focal nodular ROI within the image in rater 1 (1.7% vs. 13.4%, $p<0.001$) and in rater 2 (1.4% vs. 16.9%, $p<0.001$) and in different images in rater 1 (7.6% vs. 12.3%, $p=0.040$) and in rater 2 (7.5% vs. 19.8%, $p=0.004$). Moreover, CV of the interrater assay showed similar results (14.9% vs. 19%, $p=0.030$). Interrater intraclass correlation coefficient showed better agreement in total nodular ROI than in focal nodular ROI (0.863 vs. 0.783). The degree of fibrosis on histopathology showed significant correlations with EI (EMean, $p<0.001$; EMax, $p=0.027$), and the location of fibrosis was concordant with the high EI area on SWE. Conclusion Our study revealed that the new total nodular ROI method showed higher reproducibility and better agreement in intra- and interrater assay than the focal nodular ROI method, suggesting a new, valuable, and standardized method in clinical practice. Moreover, our results showed that causes the elevation of EI leading to wide discrepant cut-off values of thyroid cancer was the formation of fibrosis.

Background

A thyroid nodule is a common finding in up to 60% of the population during ultrasound (US) examination, and the malignancy rate for the thyroid nodules is 5–15% [1, 2]. Fine-needle aspiration (FNA) cytology is the first step that is performed to differentiate malignant nodules, but 5–15% of FNA revealed inadequate nondiagnostic samples, and 15–30% of FNA result in indeterminate cytologic findings category III (atypia or follicular neoplasm of undetermined significance) and category IV (suspicious for follicular neoplasm) according to the Bethesda system [3, 4]. Hence, additional tools to aid in the differentiation of malignant nodules are needed.

US elastography had been reported to be useful in the differentiation of benign and malignant thyroid nodules [5–9]. Strain elastography was initially developed with the operator using manual compression on the tissue to measure tissue displacement (strain) caused by the compression (stress) [10]. However, strain elastography had several disadvantages including the following: high operator dependence in terms of compression and absence of sufficient quantitative information [11, 12]. Shear wave elastography (SWE) uses several focused ultrasonic pushing beams to generate shear waves and measures transversely propagated shear wave speed, and subsequent ultrafast echographic imaging

sequence generates a quantitative elastogram [13]. SWE has sufficient quantitative information and is operator independent in terms of compression; hence, it is expected to be more reproducible than strain elastography, and two-dimensional SWE (2D-SWE) represents focal tissue stiffness map [14, 15]. Studies using SWE in assessing the thyroid nodules have reported that SWE was useful in detecting malignant nodules; however, it showed a wide range of cut-off values of elasticity index (EI) in detecting malignant nodules ranging from 34 kPa to 90 kPa [9, 16–25]. Thyroid nodules usually show heterogeneous images of EI within the nodule on 2D-SWE; thus, selecting different locations of region of interest (ROI) within the nodule displays different ROI even by the same operator [12, 26]. Difficulty in imaging and the subjective features of selecting representative location of ROI in thyroid nodules with heterogeneous EI produce variable EI profiles in SWE [27, 28]. Therefore, SWE is not operator dependent in terms of the added stress (compression) but operator dependent in the placement of ROI. To decrease this subjective variance in the placement of ROI in thyroid nodules, we let the total nodular area the ROI by tracing the total nodular margin using the overlapping B-mode US. To the best of our knowledge, this is the first trial that evaluates the total area of the nodule by tracing the nodular margin. We compared the reproducibility and reliability of EI between the total nodular ROI and the focal nodular ROI using 3-mm circular area.

Tissue elasticity is known to better increase in fibrosis [14] than in solid tumor formation [29]. Additionally, it has been reported that elasticity on strain elastography and SWE is increased related to fibrosis but not with cellularity in the papillary thyroid carcinoma (PTC) [30–33]. We tried to determine the pathological findings matching the high EI areas in 2D-SWE by comparing 2D-SWE of the thyroid nodule with surgical histopathology.

First, we aim to investigate the reliability and reproducibility of EI by SWE in the new total nodular ROI and compare it with EI in the focal nodular ROI to validate the adequacy of EI by SWE as a reliable parameter of stiffness. Second, we determine to study the relationship between the degree and location of fibrosis in the surgical histopathology and the magnitude and location of high EI area on 2D-SWE.

Patients And Methods

Study population

From November 2015 to May 2018, a total of 588 patients who visited the thyroid clinic of Soonchunhyang University Hospital for the evaluation of thyroid nodules and who underwent SWE before US guided FNA or core-needle biopsy were retrospectively reviewed in this study.

Among these subjects, 44 had thyroid cancer on surgical pathology. Patients with poor results in SWE including, thyroid nodules with poor shear wave mapping (n = 7) or with macrocalcifications (n = 3) and presence of nodules at the isthmic/paraisthmic areas due to the interference produced by the tracheal cartilage (n = 5) were excluded. Ultimately, the data from 29 thyroid cancers in 28 patients were included in this study. There were 24 cases of conventional type of PTC, 2 cases of follicular variant PTC, 2 cases of follicular thyroid carcinoma and 1 case of medullary thyroid carcinoma.

Gray-scale ultrasound and shear wave elastography examinations

The patients were positioned for US with their necks extended. Each patient underwent gray-scale US and SWE using the Aixplorer US system (SuperSonic Imagine, Aix-en-Provence, France) and a linear probe with a frequency range of 15–4 MHz. During gray-scale US examination, thyroid nodules were evaluated for size (width, depth and length), volume, composition, orientation, echogenicity, shape, margin, and presence or absence of calcification.

After the gray-scale US, SWE was performed by the same operator who had performed the gray-scale US using the same probe. To avoid compression artifacts, generous amount of gel was used. The probe was held static in transverse plane at the center of the nodule until the image had stabilized and after two or three cine-loop images were acquired, one representative elastogram was selected with fewest artifacts in each cine-loop image.

Total nodular ROI was determined by drawing the margin of the nodule guided by the overlaid B-mode anatomic scan with the mode of the machine setting using the Q-Box Trace program. We draw the margin of ROI avoiding the areas of macrocalcification and cystic portion. The EI of the total nodular ROI was calculated and displayed by the machine. The mean (E_{Mean}), minimum (E_{Min}), maximum (E_{Max}), and standard deviation (E_{SD}) of SWE EI values in the ROI were calculated as kPa, and 2D-SWE was color coded from dark blue (less than 36 kPa), light blue (36–72 kPa), green, yellow, to red (greater than 180 kPa). For the focal nodular ROI, the EI in 2–3 ROI using 3-mm circular area containing the stiffest area was measured. Moreover, the high EI area of the nodule where the color-coded EI showed higher EI than light blue (which is greater than 36 kPa) was traced by the manual drawing, and the area was calculated and displayed by the machine. The percentage of high EI area was calculated as follows: high EI area divided by the total nodular area. For the evaluation of interrater agreement, the second physician performed the same examination just after the first physician.

Pathological analysis

Surgical specimen was cut in coronal section in the largest diameter corresponding to the center of the nodule on 2D-SWE. Surgical histopathology was stained with hematoxylin and eosin staining and was diagnosed according to the World Health Organization classification [34]. Collagen fibers on histological slides were stained with Masson's trichrome stain. Under low-power microscopy (x12 or x40), the image of the area showing the thyroid carcinoma was taken. The area of fibrosis and the total area of the thyroid carcinoma under the low-power microscopy images were taken, and the areas were measured using Q-Box Trace program calculating the area with the irregular margin, and the percentage of fibrotic area was calculated by dividing the fibrotic area by the total area of the tumor.

Statistical analysis

The tumor size and elasticity values of all the lesions were expressed as medians (25th, 75th percentile). The differences between the thyroid carcinoma groups were compared using the Mann-Whitney U-test.

To assess reproducibility of elasticity measurement, intra- and interrater agreements were evaluated using the intraclass correlation coefficient (ICC; two-way random, absolute agreement). Agreement for interrater measurements was also analyzed using Bland-Altman plots [35–37].

The coefficient of variation (CV) was calculated by the ratio of the standard deviation and mean value. A linear regression model was analyzed examining the correlation between EI and the percent of high EI area on SWE with the degree of fibrosis on histopathology. All statistical analyses were performed using the SPSS Statistics 25.0 software package (Chicago, IL, USA). P values less than 0.05 were considered statistically significant.

Results

Intra- and Interrater Agreement of Mean Elasticity in Each Method

One representative elastogram from each cine-loop of 2 images was selected, and a total of 80 images from the 20 thyroid nodules by 2 raters from 18 subjects were obtained. The mean, SD, minimum, and maximum elasticity values of E_{Mean}, and intra- and interrater agreement for the quantitative measurements of E_{Mean} are summarized in Table 1. For the total nodular ROI method, there was good intrarater agreement of E_{Mean}, and ICC in rater 1 and rater 2 were 0.975 and 0.999 within the image and 0.959 and 0.976 in different images, respectively. The intrarater ICC of the focal nodular ROI method in rater 1 and rater 2 were 0.866 and 0.934 within the image and 0.734 and 0.894 in different images, respectively.

The first elastogram in each cine-loop was used to calculate the ICC and to assess the interrater agreement. Interrater ICC of the total nodular ROI and focal nodular ROI were 0.863 and 0.783, respectively. The intrarater CVs of the total nodular ROI method in rater 1 and rater 2 were significantly lower than that of the focal nodular ROI method in rater 1 (1.7% vs. 13.4%, $p<0.001$) and in rater 2 (1.4% vs. 16.9%, $p<0.001$) within the image and in rater 1 (7.6% vs. 12.3%, $p = 0.040$) and in rater 2 (7.5% vs. 19.8%, $p = 0.004$) in different images. The interrater CV of the total nodular ROI method was significantly lower than that of the focal nodular ROI method (14.9% vs. 19.0%, $p = 0.030$). Analysis using the Bland-Altman plots for E_{Mean} between 2 raters is shown in Fig. 1. Bland-Altman analysis between the 2 raters for the total nodular ROI method showed a bias of 0.4 and limits of agreement of −12.9 to 13.7, with a repeatability coefficient between the 2 raters of 13.3. The focal nodular ROI method showed a bias of −0.4 and limits of agreement of −16.4 to 15.6, with a repeatability coefficient between the 2 raters of 16.0.

Correlation between Elasticity Index Measurements on Shear Wave Elastography and the Degree of Fibrosis on Surgical Histopathology

To evaluate the correlation between EI measurements on SWE and the degree of fibrosis on surgical histopathology, we reviewed and compared the SWE images and the histological specimens as shown in Fig. 2. Our data showed a strong positive correlation between high EI area on SWE and the degree of fibrosis on surgical histopathology (r = 0.847, p<0.001) (Fig. 3A), and also between E_{Mean} and the degree of fibrosis on surgical histopathology (r = 0.706, p< 0.001) (Fig. 3B). E_{Max} showed a weak positive correlation with the degree of fibrosis on surgical histopathology (r = 0.419, p = 0.027) (Fig. 3C). The fibrosis on surgical histopathology was higher in conventional PTCs (Group 1) than in the non-conventional PTCs including follicular variant PTCs, follicular thyroid carcinomas, and a medullary thyroid carcinoma (Group 2). Group 1 showed higher EI values and EI area than Group 2, which were statistically significant for E_{Mean} (p = 0.012), E_{Max} (p = 0.032), E_{SD} (p = 0.016), and high EI area on SWE (p = 0.003) (Fig. 4).

Discussion

SWE is operator independent in terms of adding stress but is operator dependent in the placement of ROI, and the difficulty in images and the subjective features of selecting representative location of ROI were considered as the causes of variability of SWE [14, 27, 28].

We tried a new method of placement of ROI by tracing the total nodule and evaluated the reproducibility and compared total nodular ROI with conventional focal ROI using 3-mm circular area. The intrarater CVs of the total nodular ROI method in rater 1 and rater 2 were significantly lower than that of the focal nodular ROI method in rater 1 (1.7% vs. 13.4%, p<0.001) and in rater 2 (1.4% vs. 16.9%, p<0.001) within the image and in rater 1 (7.6% vs. 12.3%, p = 0.040) and in rater 2 (7.5% vs. 19.8%, p = 0.004) in different images. Moreover, the interrater CV of the total nodular ROI method was significantly lower than that of the focal nodular ROI method (14.9% vs. 19.0%, p = 0.030). Bardet et al. [26] reported that the intra- and interobserver CVs for the mean EI in the focal nodular ROI were 23% and 26%, respectively. Brezak et al. [38] reported that the intra- and interreader CVs in the focal nodular ROI for the mean EI were 13% and 21%, respectively, and both reports were compatible with our results for the focal nodular ROI.

Moreover, the agreement of the mean EI between the total and focal nodular area ROI was evaluated by ICC in this study. The mean EI in the total nodular ROI showed better agreement than in the focal nodular ROI in intra-assay agreement (ICC, 0.959 vs. 0.894 in rater 1 and 0.976 vs. 0.734 in rater 2) and also in interrater agreement (ICC, 0.863 vs. 0.783). Bland-Altman plot analysis of interrater agreement showed better interrater agreement of EI in the total nodular ROI than in the focal nodular ROI. Our study revealed SWE EI measurement in the total nodular ROI was more reproducible and showed less variability

compared to the mean EI in the focal nodular ROI and suggested that it may be a valuable and standardized method in clinical practice.

By comparing EI with the degree of fibrosis, E_{Mean} and E_{Max} showed a correlation with the percent of fibrosis. Additionally, comparison of EI with surgical histopathology revealed that high EI areas in SWE in thyroid cancer were concordant to the areas of fibrosis. PTC is commonly associated with fibrotic change particularly evident at the advancing edge [34] and up to 80% of PTC showed fibrotic change with various degrees [39, 40], while stromal component of follicular neoplasm especially adenoma is typically scant [34] and occasionally shows stromal fibrosis and hemorrhage [40]. Regarding follicular thyroid carcinoma, several studies reported that SWE did not show significantly elevated elasticity [7, 20] similar to benign nodules. Rago et al. [30] reported that the elasticity of the thyroid nodules with stain elastography did not correlate with cell number, and nodule stiffness was correlated with the degree of fibrosis, which was more evident in classic PTC than in follicular variant PTC. Yi et al. [31] reported that the strain ratio of US elastography was positively correlated with the degree of fibrosis of PTC on surgical histopathology. Fukuhara et al. [32, 33] reported that when malignant thyroid nodules were classified according to the degree of fibrosis on histopathology, SWE showed high shear wave velocity in nodules with severe fibrosis and malignant nodules with no fibrosis showing similar shear wave velocity with benign nodules with no fibrosis, and the effect of cell density on shear wave velocity was insignificant. These reports suggest that fibrosis plays a major role in the elasticity of the thyroid nodules, and elevated elasticity in thyroid cancer is mainly related with fibrosis, which is frequent in PTC and non-conventional PTC with less or no fibrosis showing insignificant or slight elevation of elasticity including follicular carcinoma and follicular variant PTC [25, 26]. Our study that showed E_{Mean} was significantly higher in conventional PTC than in non-conventional PTC, which is similar to the results of the other studies. Our data revealed that the percentage of high EI (greater than 36 kPa) area of the nodule showed a correlation with the degree of fibrosis (percentage of fibrosis on surgical histopathology); moreover, EI (E_{Max} and E_{Mean}) was correlated with the degree of fibrosis. Additionally, the location of fibrosis was concordant with high EI area. Hence, the degree and location of fibrosis on histopathology were closely correlated with the high EI of the thyroid nodule. Diverse elasticity in PTC may reflect various degrees of fibrosis in PTC, resulting in the discrepant cut-off values in the diagnosis of malignant thyroid nodules, because more than 80% of malignant nodules are composed of PTC. A wide range of cut-off values of EI in detecting malignancy from 34 kPa to 90 kPa was reported [9, 16–25], and which may be due to the various degrees of fibrosis in different patients and different types of tumors in the same study and also in the different study groups.

Conclusions

Our study revealed that the mean EI in the total nodular ROI showed higher reproducibility and better agreement in intra- and interrater assay than in the focal nodular ROI when evaluating the ICC, CV, and Bland-Altman analysis, which may be due to the folloing reason: avoidance of the subjective variance of placement of ROI in the focal nodular area. We suggest that the total nodular ROI method may be a

valuable and standardized method in clinical practice. Our results showed that fibrosis increased SWE elasticity in the histopathology of the thyroid nodule, which might lead to the discrepancy of the cut-off values in detecting thyroid cancer. A limitation of this study is the relatively small number of non-conventional PTC, and a future study with larger numbers may be needed for further clarification of the possible characteristic features of SWE in non-PTC.

Abbreviations

US: ultrasound; FNA: fine-needle aspiration cytology; SWE: shear wave elastography; EI: elasticity index; ROI: region of interest; PTC: papillary thyroid carcinoma; CNB: core-needle biopsy; E_{Mean}: mean elasticity; E_{Min}: minimum elasticity; E_{Max}: maximum elasticity; E_{SD}: one standard deviation of elastographic values; ICC: intraclass correlation coefficient; CV: coefficient of variation.

Declarations

Acknowledgments

We would like to thank the research coordinator Maeja Kim, from the Soonchunhyang University Hospital for her help in data collection.

Funding

This work was supported by the Soonchunhyang University Research Fund. None of the funding sources were involved in design of the study, data collection and analysis, interpretation of results, writing of the manuscript, or in the decision to submit the manuscript for publication.

Availability of data and material

The datasets used and analyzed in the current study are available from the corresponding author on reasonable request.

Authors’ contributions

MHY analyzed and interpreted study concepts. MHY, HJK and SYP analyzed and interpreted study design. HJK and IHC obtained the data. SJK, HKP and DWB controlled the quality of data and algorithms. HJK and SYP conducted the statistical analysis. MHY and HJK prepared and edited for the manuscript. IHC, SJK, HKP, DWB and KS reviewed the manuscript for critical revisions.

Ethics approval and consent to participate

The Institutional Review Board of Soonchunhyang University Hospital approved the study (approval no. 2018–11–019). The requirement for informed consent for this study was waived by the institutional review board because researchers only accessed the database for analysis purposes and personal identifying information was not accessed.

Consent for publication

Not applicable.

Competing interests

The authors have no competing interests to disclose.

References

1.Bongiovanni M, Spitale A, Faquin WC, Mazzucchelli L, Baloch ZW: *The Bethesda System for Reporting Thyroid Cytopathology: a meta-analysis. Acta cytologica* 2012, *56(*4):333–339.

2.Mazzaferri EL: *Management of a solitary thyroid nodule. The New England journal of medicine* 1993, *328(*8):553–559.

3.Cibas ES, Ali SZ: *The 2017 Bethesda System for Reporting Thyroid Cytopathology. Thyroid: official journal of the American Thyroid Association* 2017, *27(*11):1341–1346.

4.Alexander EK: *Approach to the patient with a cytologically indeterminate thyroid nodule. The Journal of clinical endocrinology and metabolism* 2008, *93(*11):4175–4182.

5.Rago T, Santini F, Scutari M, Pinchera A, Vitti P: *Elastography: new developments in ultrasound for predicting malignancy in thyroid nodules. The Journal of clinical endocrinology and metabolism* 2007, *92(*8):2917–2922.

6.Ragazzoni F, Deandrea M, Mormile A, Ramunni MJ, Garino F, Magliona G, Motta M, Torchio B, Garberoglio R, Limone P: *High diagnostic accuracy and interobserver reliability of real-time elastography in the evaluation of thyroid nodules. Ultrasound in medicine & biology* 2012, *38(*7):1154–1162.

7.Asteria C, Giovanardi A, Pizzocaro A, Cozzaglio L, Morabito A, Somalvico F, Zoppo A: *US-elastography in the differential diagnosis of benign and malignant thyroid nodules. Thyroid: official journal of the American Thyroid Association* 2008, *18(*5):523–531.

8.Azizi G, Keller J, Lewis M, Puett D, Rivenbark K, Malchoff C: *Performance of elastography for the evaluation of thyroid nodules: a prospective study. Thyroid: official journal of the American Thyroid Association* 2013, *23(*6):734–740.

9.Sebag F, Vaillant-Lombard J, Berbis J, Griset V, Henry JF, Petit P, Oliver C: *Shear wave elastography: a new ultrasound imaging mode for the differential diagnosis of benign and malignant thyroid nodules. The Journal of clinical endocrinology and metabolism* 2010, *95(*12):5281–5288.

10.Gennisson JL, Deffieux T, Fink M, Tanter M: *Ultrasound elastography: principles and techniques. Diagnostic and interventional imaging* 2013, *94(*5):487–495.

11.Kamaya A, Machtaler S, Safari Sanjani S, Nikoozadeh A, Graham Sommer F, Pierre Khuri-Yakub BT, Willmann JK, Desser TS: *New technologies in clinical ultrasound. Seminars in roentgenology* 2013, *48(*3):214–223.

12.Garra BS: *Imaging and estimation of tissue elasticity by ultrasound. Ultrasound quarterly* 2007, *23(*4):255–268.

13.Athanasiou A, Tardivon A, Tanter M, Sigal-Zafrani B, Bercoff J, Deffieux T, Gennisson JL, Fink M, Neuenschwander S: *Breast lesions: quantitative elastography with supersonic shear imaging—preliminary results. Radiology* 2010, *256(*1):297–303.

14.Sigrist RMS, Liau J, Kaffas AE, Chammas MC, Willmann JK: *Ultrasound Elastography: Review of Techniques and Clinical Applications. Theranostics* 2017, *7(*5):1303–1329.

15.Garra BS: *Elastography: history, principles, and technique comparison. Abdominal imaging* 2015, *40(*4):680–697.

16.Wang F, Chang C, Chen M, Gao Y, Chen YL, Zhou SC, Li JW, Zhi WX: *Does Lesion Size Affect the Value of Shear Wave Elastography for Differentiating Between Benign and Malignant Thyroid Nodules? Journal of ultrasound in medicine: official journal of the American Institute of Ultrasound in Medicine* 2018, *37(*3):601–609.

17.Azizi G, Keller JM, Mayo ML, Piper K, Puett D, Earp KM, Malchoff CD: *Shear wave elastography and Afirma gene expression classifier in thyroid nodules with indeterminate cytology: a comparison study. Endocrine* 2018, *59(*3):573–584.

18.Duan SB, Yu J, Li X, Han ZY, Zhai HY, Liang P: *Diagnostic value of two-dimensional shear wave elastography in papillary thyroid microcarcinoma. OncoTargets and therapy* 2016, *9:*1311–1317.

19.Gregory A, Bayat M, Kumar V, Denis M, Kim BH, Webb J, Meixner DD, Ryder M, Knudsen JM, Chen S *et al: Differentiation of Benign and Malignant Thyroid Nodules by Using Comb-push Ultrasound Shear Elastography: A Preliminary Two-plane View Study. Academic radiology* 2018, *25(*11):1388–1397.

20.Veyrieres JB, Albarel F, Lombard JV, Berbis J, Sebag F, Oliver C, Petit P: *A threshold value in Shear Wave elastography to rule out malignant thyroid nodules: a reality? European journal of radiology* 2012, *81(*12):3965–3972.

21.Kim H, Kim JA, Son EJ, Youk JH: *Quantitative assessment of shear-wave ultrasound elastography in thyroid nodules: diagnostic performance for predicting malignancy. European radiology* 2013, *23(*9):2532–2537.

22.Park AY, Son EJ, Han K, Youk JH, Kim JA, Park CS: *Shear wave elastography of thyroid nodules for the prediction of malignancy in a large scale study. European journal of radiology* 2015, *84(*3):407–412.

23.Liu Z, Jing H, Han X, Shao H, Sun YX, Wang QC, Cheng W: *Shear wave elastography combined with the thyroid imaging reporting and data system for malignancy risk stratification in thyroid nodules. Oncotarget* 2017, *8(*26):43406–43416.

24.Chang N, Zhang X, Wan W, Zhang C, Zhang X: *The Preciseness in Diagnosing Thyroid Malignant Nodules Using Shear-Wave Elastography. Medical science monitor: international medical journal of experimental and clinical research* 2018, *24:*671–677.

25.Bhatia KS, Tong CS, Cho CC, Yuen EH, Lee YY, Ahuja AT: *Shear wave elastography of thyroid nodules in routine clinical practice: preliminary observations and utility for detecting malignancy. European radiology* 2012, *22(*11):2397–2406.

26.Bardet S, Ciappuccini R, Pellot-Barakat C, Monpeyssen H, Michels JJ, Tissier F, Blanchard D, Menegaux F, de Raucourt D, Lefort M *et al: Shear Wave Elastography in Thyroid Nodules with Indeterminate Cytology: Results of a Prospective Bicentric Study. Thyroid: official journal of the American Thyroid Association* 2017, *27(*11):1441–1449.

27.Swan KZ, Nielsen VE, Bibby BM, Bonnema SJ: *Is the reproducibility of shear wave elastography of thyroid nodules high enough for clinical use? A methodological study. Clinical endocrinology* 2017, *86(*4):606–613.

28.Anvari A, Dhyani M, Stephen AE, Samir AE: *Reliability of Shear-Wave Elastography Estimates of the Young Modulus of Tissue in Follicular Thyroid Neoplasms. AJR American journal of roentgenology* 2016, *206(*3):609–616.

29.Hedrick W: *Technology for diagnostic sonography.* St Louis: Elsevier Mosby; 2013.

30.Rago T, Scutari M, Loiacono V, Santini F, Tonacchera M, Torregrossa L, Giannini R, Borrelli N, Proietti A, Basolo F *et al: Low Elasticity of Thyroid Nodules on Ultrasound Elastography Is Correlated with Malignancy, Degree of Fibrosis, and High Expression of Galectin–3 and Fibronectin–1. Thyroid: official journal of the American Thyroid Association* 2017, *27(*1):103–110.

31.Yi L, Qiong W, Yan W, Youben F, Bing H: *Correlation between Ultrasound Elastography and Histologic Characteristics of Papillary Thyroid Carcinoma. Scientific reports* 2017, *7:*45042.

32.Fukuhara T, Matsuda E, Endo Y, Takenobu M, Izawa S, Fujiwara K, Kitano H: *Correlation between quantitative shear wave elastography and pathologic structures of thyroid lesions. Ultrasound in medicine & biology* 2015, *41(*9):2326–2332.

33.Fukuhara T, Matsuda E, Endo Y, Donishi R, Izawa S, Fujiwara K, Kitano H, Takeuchi H: *Impact of Fibrotic Tissue on Shear Wave Velocity in Thyroid: An Ex Vivo Study with Fresh Thyroid Specimens. BioMed research international* 2015, *2015:*569367.

34.Lloyd RV, Osamura RY, Kloppel G, Rosai J: *WHO Classification of Tumours of Endocrine Organs,* 4th edn. Lyon, France: IARC Press; 2017.

35.Bland JM, Altman DG: *A note on the use of the intraclass correlation coefficient in the evaluation of agreement between two methods of measurement. Computers in biology and medicine* 1990, *20(*5):337–340.

36.Kottner J, Audige L, Brorson S, Donner A, Gajewski BJ, Hrobjartsson A, Roberts C, Shoukri M, Streiner DL: *Guidelines for Reporting Reliability and Agreement Studies (GRRAS) were proposed. Journal of clinical epidemiology* 2011, *64(*1):96–106.

37.Bland JM, Altman DG: *Statistical methods for assessing agreement between two methods of clinical measurement. Lancet (London, England)* 1986, *1(*8476):307–310.

38.Brezak R, Hippe D, Thiel J, Dighe MK: *Variability in Stiffness Assessment in a Thyroid Nodule Using Shear Wave Imaging. Ultrasound quarterly* 2015, *31(*4):243–249.

39.Koperek O, Asari R, Niederle B, Kaserer K: *Desmoplastic stromal reaction in papillary thyroid microcarcinoma. Histopathology* 2011, *58(*6):919–924.

40.Kumar V, Abbas AK, Aster JC: *Robbins and Cotran Pathologic Basis of Disease,* 9th edn. Philadelphia, PA; 2015.

Table

Method of ROI	E_{Mean} (kPa), mean ± SD (min-max)		ICC (95% CI)	CV (%)
	Read 1	Read 2		
Total nodular ROI				
Intrarater assay (within image)				
Rater 1	25.3 ± 10.0 (12.0-49.6)	24.7 ± 9.0 (12.1-40.1)	0.975 (0.983-0.990)	1.7
Rater 2	24.3 ± 11.7 (9.6-58.7)	24.3 ± 11.9 (9.2-59.9)	0.999 (0.997-1.000)	1.4
Intrarater assay (different image)				
Rater 1	24.8 ± 9.0 (12.0-40.0)	24.6 ± 9.4 (9.3-41.7)	0.959 (0.895-0.984)	7.6
Rater 2	24.3 ± 11.7 (9.6-58.7)	26.0 ± 13.1 (10.3-60.8)	0.976 (0.933-0.991)	7.5
Interrater assay	25.3 ± 10.0 (12.0-49.6)	24.3 ± 11.7 (9.6-58.7)	0.863 (0.653-0.946)	14.9
Focal nodular ROI				
Intrarater assay (within image)				
Rater 1	34.0 ± 17.2 (14.4-86.3)	39.6 ± 22.9 (16.3-115.2)	0.934 (0.842-0.973)	13.4
Rater 2	45.0 ± 36.8 (12.4-179.9)	36.6 ± 23.4 (10.4-111.8)	0.866 (0.693-0.945)	16.9
Intrarater assay (different image)				
Rater 1	34.0 ± 17.2 (14.4-86.3)	33.6 ± 11.9 (11.2-53.7)	0.894 (0.730-0.958)	12.3
Rater 2	45.0 ± 36.8 (12.4-179.9)	37.1 ± 19.1 (11.1-93.1)	0.734 (0.347-0.894)	19.8
Interrater assay	34.0 ± 17.2 (14.4-86.3)	45.0 ± 36.8 (12.4-179.9)	0.783 (0.443-0.915)	19.0

Table 1. Shear wave elasticity values, and intra- and interrater intraclass correlation coefficient (ICC) agreement and coefficient of variation (CV) for E_{Mean} (mean elasticity) in region of interest (ROI) with the two methods (total nodular ROI with tracing total nodule and focal nodular ROI with 3 mm circle) by two raters.

Figures

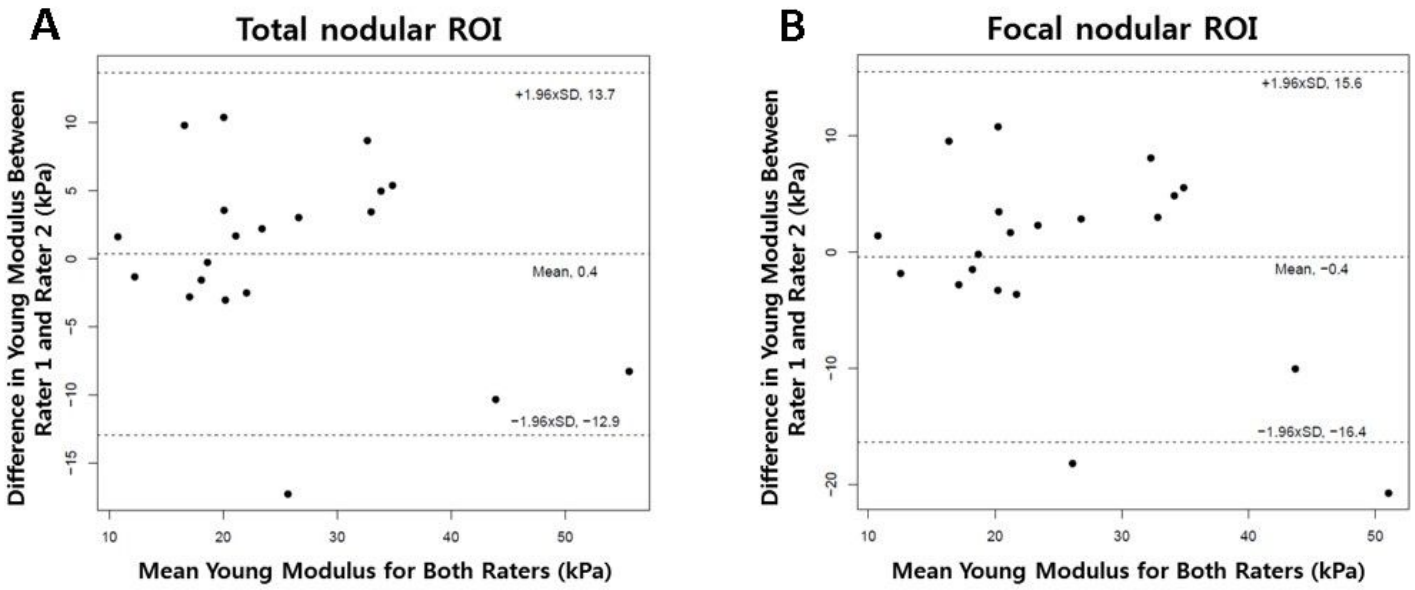

Figure 1

Bland-Altman plot of Young Modulus (EMean) between two raters. (A) Total nodular ROI. (B) Focal nodular ROI. EMean, mean elasticity; ROI, region of interest; kPa, kilo-Pascal

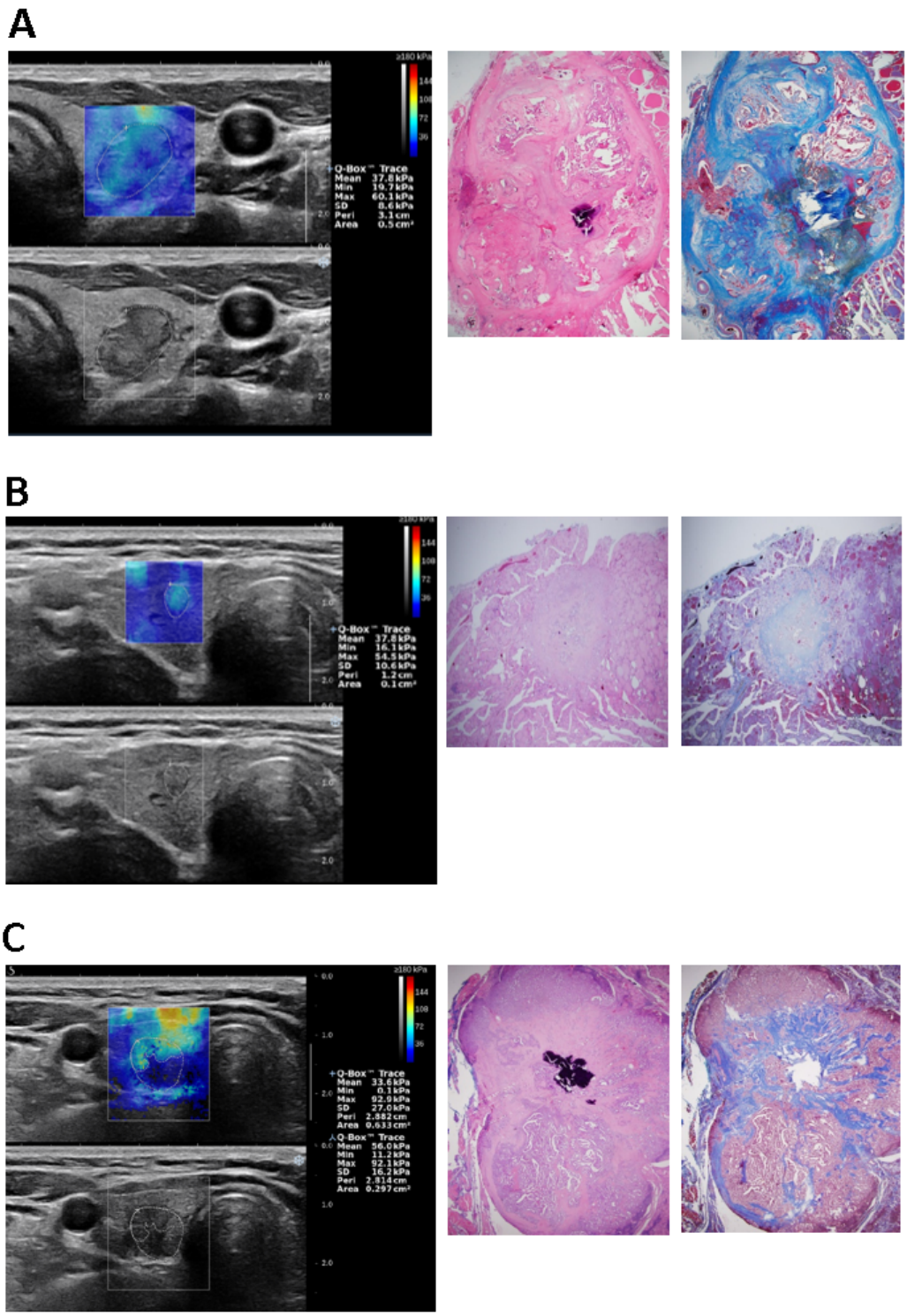

Figure 2

Shear wave elastography (SWE), gray-scale ultrasound (US), H&E staining, and Masson's trichrome staining slides of the papillary thyroid carcinoma in 3 patients. (A) The case is from a 44-year-old patient with a 1.63-cm left middle thyroid nodule. A suspicious malignant nodule with hypoechogenicity and lobulated margin was observed on gray-scale US. SWE showed generalized uneven distribution of high elasticity index (EI) area within the nodule. Masson's trichrome staining showed uneven irregular

distribution of fibrosis within the nodule, concordant with the high EI area on SWE. (B) The case is from a 63-year-old patient with a 0.52-cm right middle thyroid nodule. A suspicious malignant nodule with taller-than-wide shape, microcalcification, and irregular margin was observed on gray-scale US. SWE showed high EI area over the entire nodule. On Masson Trichrome staining, fibrosis was observed in the entire nodule, concordant with the high EI area on SWE. (C) The case is from a 53-year-old patient with a 1.00-cm right lower thyroid nodule. A suspicious malignant nodule with hypoechogenicity, microcalcification, and lobulated margin was observed on gray-scale US. SWE showed high EI area in the upper portion of the nodule. Similar to the high EI area on SWE, fibrosis was observed in the upper portion of the nodule on Masson's trichrome staining.

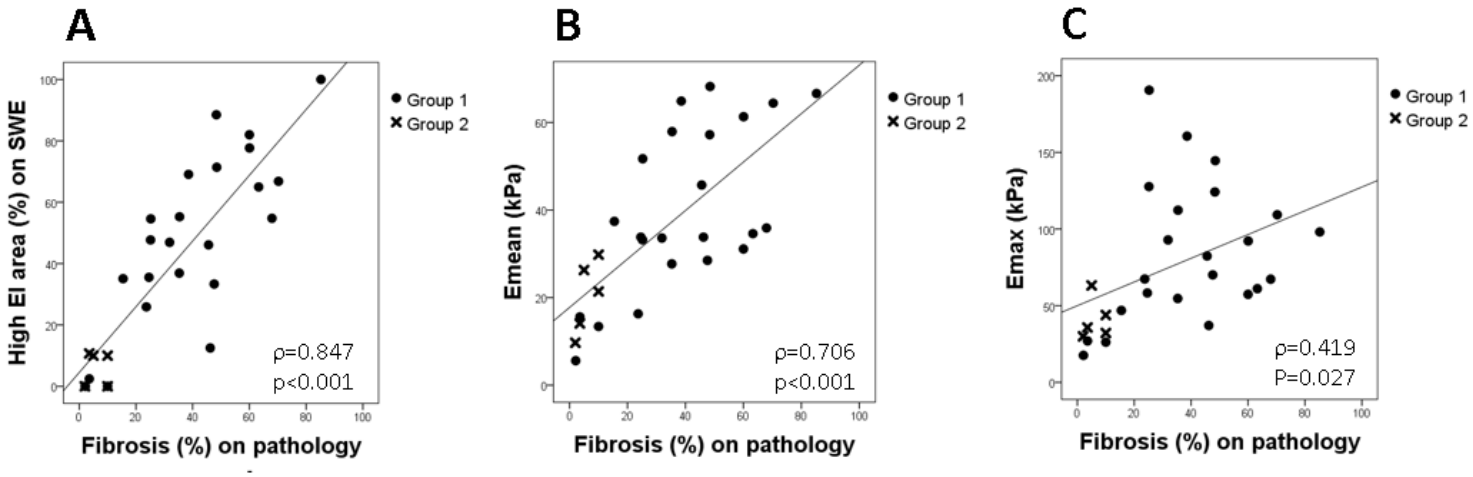

Figure 3

Correlation between elasticity index (EI) measurements on shear wave elastography (SWE) and the degree of fibrosis on surgical histopathology. (A) high EI area on SWE. (B) EMean. (C) EMax. Group1, conventional type of papillary thyroid carcinoma (n=24); Group 2, non-conventional papillary thyroid carcinoma including follicular variant of papillary thyroid carcinoma (n=2), follicular thyroid carcinoma (n=2), and medullary thyroid carcinoma (n=1). EMean, mean elasticity; EMax, maximum elasticity; kPa, kilo-Pascal.

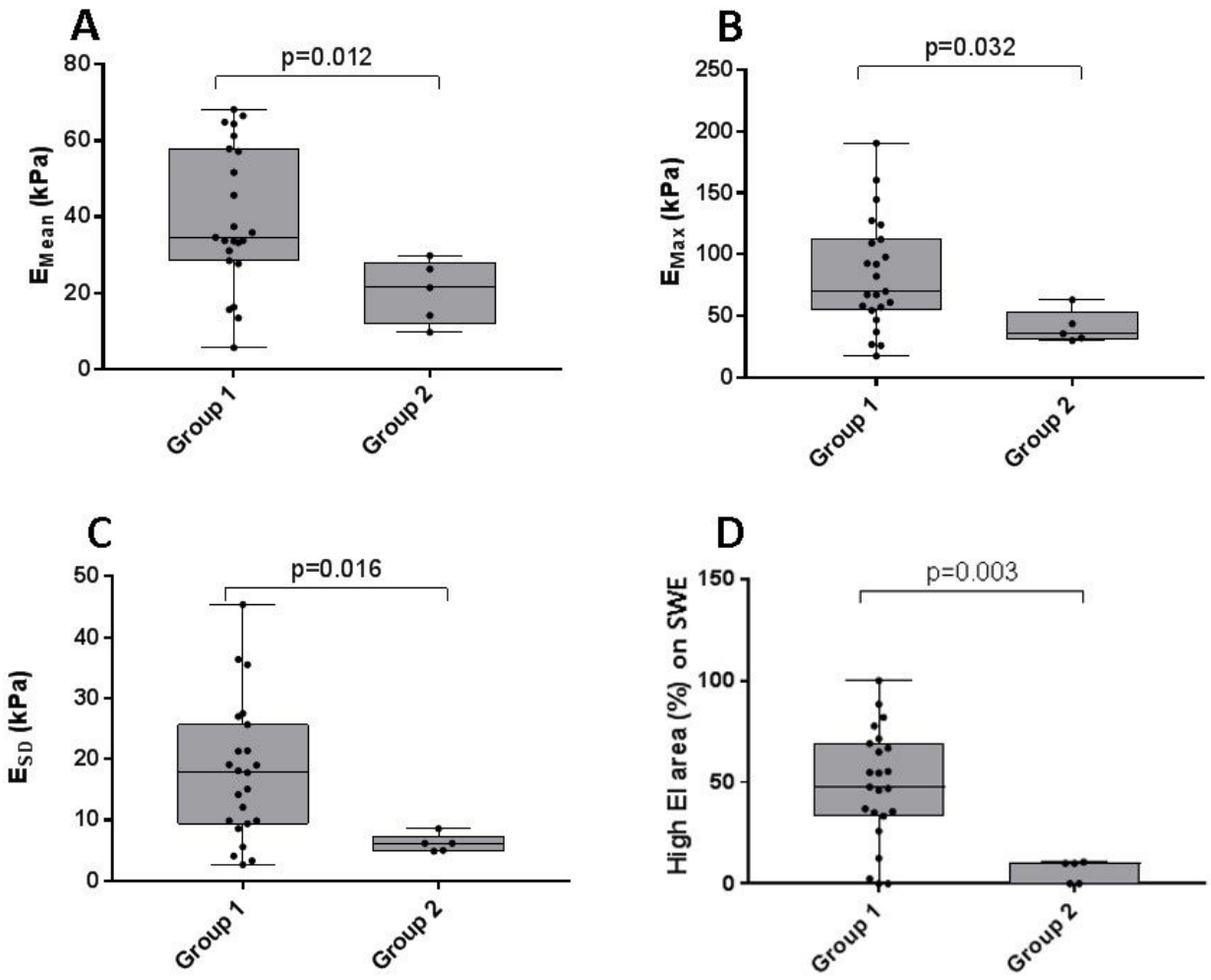

Figure 4

Box-and-whisker plots of elasticity index (EI) measurements on shear wave elstography (SWE) for group 1 and group 2. (A) EMean. (B) EMax. (C) ESD. (D) high EI area on SWE. Group1, conventional type of papillary thyroid carcinoma (n=24); Group 2, non-conventional papillary thyroid carcinoma (n=5) including follicular variant of papillary thyroid carcinoma (n=2), follicular thyroid carcinoma (n=2), and medullary thyroid carcinoma (n=1); EMean, mean elasticity; EMax, maximum elasticity; ESD, one standard deviation of elastographic values; kPa, kilo-Pascal.